Uzbek Journal of Physics

Vol.20(№4) 2018 PP.218-223

PSEUDOMORPHIC GeSiSn LAYERS IN STRAINED HETEROSTRUCTURES

A.I. Nikiforov[1,2], V.A. Timofeev[1], A.I. Yakimov[1,2], V.I. Mashanov[1], I.D. Loshkarev[1], A.K. Gutakovskii[1], O.P. Pchelyakov[1,2], Kh.B. Ashurov[3]

[1]Rzhanov Institute of Semiconductor Physics, Siberian Branch of the Russian Academy of Sciences, Lavrentjeva 13, 630090 Novosibirsk, Russia, nikif@isp.nsc.ru
[2]National Research Tomsk State University, 36, Lenina Avenue, Tomsk, 634050, Russia
[3]Arifov Institute of Ion-Plasma and Laser Technologies, Uzbekistan Academy of Sciences, 100125 Tashkent, Uzbekistan

Проведены исследования образования псевдоморфных слоев GeSiSn непосредственно на кремнии. Изучен переход от двумерного механизма роста к трехмерному пленки GeSiSn на поверхности Si(100) в зависимости от несоответствия параметров решетки и температуры роста. Показана возможность синтеза многослойных гетероструктур методом молекулярно-лучевой эпитаксии. Изменение параметра решетки контролировали методами высокоразрешающей электронной микроскопии и рентгеновской дифрактометрии. Созданы *p-i-n*-диоды на основе многослойных структур GeSiSn/Si, на которых продемонстрировано увеличение фоточувствительности, на несколько порядков величины превышающее значение в диодах без слоев с оловом. Фоточувствительность *p-i-n*-диодов увеличивалась с увеличением содержания олова. На наноструктурах на основе слоев GeSiSn обнаружена фотолюминесценция с максимумом в диапазоне 0.6–0.85 eV.

The formation of pseudomorphous GeSiSn layers directly on Si have been investigated. The transition from two-dimensional growth regime to three-dimensional of the GeSiSn film on Si(100) was studied for different mismatch with silicon and growth temperatures. A possibility of synthesis of multilayer structures by molecular beam epitaxy was shown. The crystal lattice constants were determined using the high-resolution transmission electron microscopy and X-ray diffractometry. The *p-i-n*-diodes based on multilayer GeSiSn/Si structures were created which demonstrated the photoresponse increasing by several orders of magnitude in comparison the Sn-free structures at an increase in the Sn content. Nanostructures based on GeSiSn layers have demonstrated the photoluminescence at 0.6–0.85 eV.

I. INTRODUCTION

Integration of III-V compound-based laser diodes directly on Si is difficult due to the difference in thermal expansion coefficients of III-V materials and Si. This problem, among others, hampers the combination of electronic and photonic components on a single plate. Synthesis of a direct-band IV group material on the basis of Ge-Si-Sn material opens the way to the creation of lasers and to the solution of problems of the integration of the optoelectronics and traditional silicon integrated circuits on a single chip.

Models of nanoelectronic devices (field effect and tunnel field effect transistors) and photonics (emitting devices) working on Ge-Si-Sn materials [1-4] have been recently developed and presented. Progress in the field of Ge-Si-Sn materials allows high-quality crystalline films to be grown using pseudomorphic and relaxed buffer GeSn and GeSiSn layers [5-10]. The use of tensile or compressive biaxial strains leads to a change in the band structure and allows the energy spectrum of charge carriers to be controlled. The effect of stresses on the band structure of GeSn was studied [11].

The transition to a direct gap material is thought to occur at the Sn content of ca. 9% in the cubic GeSn lattice [12, 13] but at less than 6% when the tensile strain is used. In the films with the compressive strain, the transition can only be observed at the concentrations of ca. 11% [14]. Apart from changing the electronic and optical properties, the presence of Sn on the surface results in an increase in the surface diffusion of adatoms [15] and influences the appearance of a superstructure series, which are not observed in the GeSi system [16]. The main problems of the synthesis of epitaxial GeSn and GeSiSn films are associated with a low equilibrium solubility of Sn in Ge and Si (<1%), segregation and precipitation are solved using the non-equilibrium growth techniques such as molecular beam epitaxy (MBE), magnetron sputtering, solid epitaxy, recrystallization and gas-phase epitaxy (CVD) [17-19].

The main advantage of pseudomorphic layers against thick layers is that they are free of dislocations and coherent with the substrate. The GeSiSn films are more thermally stable than GeSn [20] and have independent adjustment of the lattice parameter and band gap. We synthesized high crystalline quality GeSiSn/Si heterostructures; our structures exhibit photoluminescence with the maximum intensity from 0.77 eV to 0.65 eV.

II. EXPERIMENTAL

An MBE installation Katun-C equipped with two electron beam evaporators for Si and Ge was used for synthesis. Sn, B and Sb were evaporated from effusion cells. When triple GeSiSn compounds were grown, germanium also was evaporated from an effusion cell. The base pressure of the MBE system was 1×10^{8} Pa. Ultrahigh vacuum MBE was used for synthesis of the structures containing pseudomorphous GeSiSn layers of different compositions (0 to 10% of Sn) and thicknesses (2 to 3.5 nm). The temperature and growth rates of GeSiSn layers were varied between 100–150°C and 0.075–0.43 ML/s (1 Sn ML on Si(100) = 0.184 nm), respectively. GeSiSn layers were grown over Si at 500°C. Changes in the surface morphology and structure during GeSiSn and Si film growth were controlled using reflection high energy electron diffraction (RHEED).

The moment of 2D-3D transition was determined from the time dependent RHEED intensity along one of strains where a voluminous reflex appeared. The crystal structure of growing layers was studied using high-resolution transmission electron microscopy (TEM) with an electron microscope JEOL-4000EX (electron energy 400 keV, resolution 0.165 nm). TEM images were processes using digital micrograph software. Imaging and quantitative measurement of the lattice distortions and deformation fields were carried out by the method of geometrical phase.

P-*i*-*n*-structures with pseudomorphous GeSiSn layers in the *i*-region were grown to study electrophysical properties. The structure was grown on a doped n^{+}-Si substrate with 0.01 ohm·cm resistivity. The upper contact layer p^{+}-Si was 300 nm thick with the boron acceptor concentration $p=5\times10^{18}$ cm^{-3}. Round mesa-shaped samples of 3–4 mm in diameter were obtained in vacuum using chemical etching and spraying of aluminum contacts. Vertical photocurrent spectra were acquired with an IR Fourier spectrometer VERTEX 70 from Bruker. The optical properties of the structures are studied by photo-luminescence spectroscopy (PL). They used a monochromator ACTON 2300i and cooled OMA-V detector based on line-of InGaAs photodiodes with sensitivity band from 1.1 to 2.2 microns. For photoluminescence excitation Nd:YAG (532 nm) laser is used .

III. RESULTS AND DISCUSSION

Synthesis of multilayer structures comprising elastically strained pseudomorphous GeSiSn layers required dependences of the 2D-3D transition thickness on temperature and compositions of the GeSiSn films to be studied at various lattice misfits. The approach was similar to that used for studying pure germanium growth on Si(100) [16]. A kinetic diagram of GeSiSn growth at misfit from 1 to 5% is shown in Fig. 1. Generally, an increase in the critical thickness of 2D-3D transition is observed with a decrease of the misfit. The thickness of the pseudomorphous GeSiSn film was determined based on the growth diagrams. The two extremes near 250 and 325°C are clearly visible on the curve for the misfit of 2%. The change of the superstructure takes place in the region between the first and second extremum, which reduces the stress accumulated in the film and critical thickness of the 2D-3D transition increases. Sn collects on the surface above 325°C due to the segregation [21] and we observe the 2D-3D transition for the layer having the composition close to a double compound with a reduced concentration of Sn at 450°C. The segregation of Sn at the surface of the film depends on the growth temperature, the Sn content and also misfit of lattice parameters of GeSiSn and Si. The decrease of the Sn content in the triple compound increases the threshold value of the growth temperature at which begins the segregation of Sn. The GeSiSn growth temperature was chosen to meet the epitaxial growth conditions and to suppress Sn segregation. The optimal temperature of GeSiSn deposition was established to range from 100 to 250°C. By reducing the mismatch of GeSiSn and Si lattice parameters up to 1% (Fig. 1), the thickness of the pseudomorphic GeSiSn film can reach about 6 nm at low temperatures.

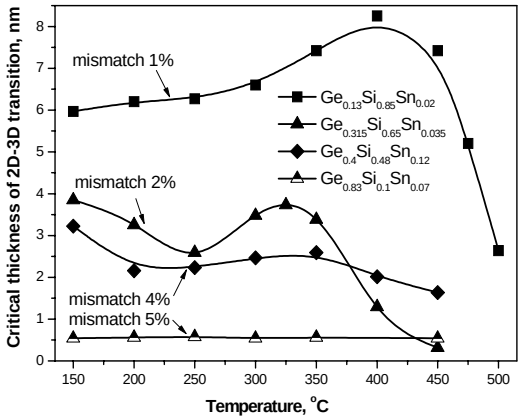


Fig. 1. Temperature dependence of the 2D-3D transition for GeSiSn films with Ge content: 13, 31.5, 40 and 83% for mismatch with Si from 1 to 5%.

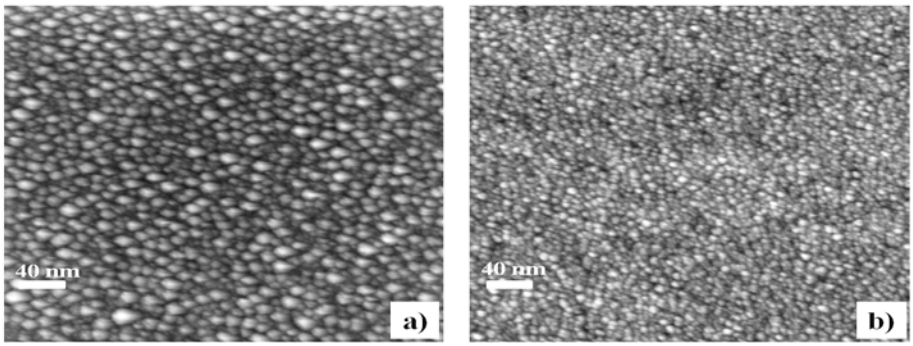


Fig. 2. STM images of the $Ge_{0.75}Si_{0.2}Sn_{0.05}$ surface with the scan size of 400×400 nm: in the first period (*a*); in the fifth period (*b*).

Periodic structures, containing pseudomorphic layers or a GeSiSn nanoisland array, were obtained. Using the kinetic diagrams of GeSiSn film morphological state, a GeSiSn island array in the multilayer periodic structure was investigated. The STM pictures of $Ge_{0.75}Si_{0.2}Sn_{0.05}$ surface with the nanoisland array in the first (Fig. 2*a*) and in the fifth periods (Fig. 2*b*) with a scan size of 400×400 nm are presented. The island array was obtained at the growth temperature of 250°C.

The pseudomorphous GeSiSn layer was then grown over by a 5–20 nm thick silicon layer at 500°C. The thickness of Si was chosen to obtain a smooth surface. A series of superstructures similar to those observed during the growth of pure tin submonolayer [22] was a result of tin segregation on the surface during the growth of Si over GeSiSn. The (4×4) superstructure is typical of the Si surface over GeSiSn layers through all the periods of the multilayer GeSiSn/Si heterostructure at the 3 to 10% Sn content and the covering growth temperature of 500°C. As the Sn content increases to above 10% at Si growing over GeSiSn, a two-domain superstructure (5×1) becomes observed. The (5×1) superstructure is typically observed at a higher Sn covering on Si(100) and, hence, indicates strengthening of the Sn segregation effect to the surface. Reduction of the temperature of covering growth prevents the segregation phenomenon and smoothens the roughness of the Si film over the GeSiSn layer. TEM was used to characterize the crystal perfection of the heterostructures under study (Fig. 3). Inspection of Fig. 2 leads to conclude that the structures are free of dislocations and crystal-perfect.

The crystal lattice distortions and deformation fields were visualized and measured in the TEM images of the multilayer structures GeSiSn/Si using the method of geometric phase. The experimentally measured interplanar distances (d_{002}=0.29 nm, d_{111}=0.32 nm, d_{220}=0.192 nm) (with the sample presented in Fig. 6 as an example) are to show that the tetragonal lattice with constants $a = 0.543$ nm and $c = 0.58$ nm is characteristic of GeSiSn layers. We find constant of GeSiSn cubic lattice as equal to 0.562 nm. The lattice constant is 0.5% different from the initial value preset before starting the growth of the multilayer structure.

We also studied the structure using X-ray diffractometry. Figure 4 shows one of the experimental rocking curves for a multilayer structure with the GeSiSn/Si heterojunction. The substrate gives the maximal peak. Furthermore, there are observed satellites characterizing periodicity of the multilayer structure and the thickness oscillations related

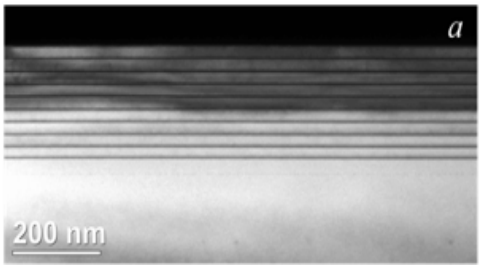


Fig. 3. TEM image of $Ge_{0.5}Si_{0.45}Sn_{0.05}$/Si heterostructure with period 25 nm.

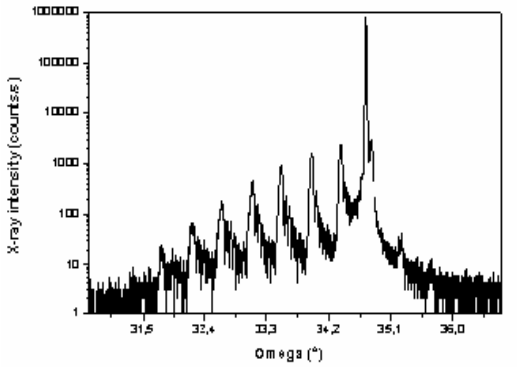


Fig. 4. XRD rocking-curve measurements of multilayer $Ge_{0.5}Si_{0.45}Sn_{0.05}$/Si heterostructures performed along symmetric (004) plane.

to the layers in the period. The observation of satellites for more than 3 orders (zero order and more than 3 orders aside) indicates quite strict periodicity in composition and thickness of the layers. The presence of thickness oscillations confirms the high quality heteroboundaries in the structure.

The *p-i-n*-structures shown in Fig. 5 were fabricated to investigate the electrophysical properties of multilayer periodic structures with pseudomorphous GeSiSn layers. The result of photoelectric measurements is presented in Fig. 6.

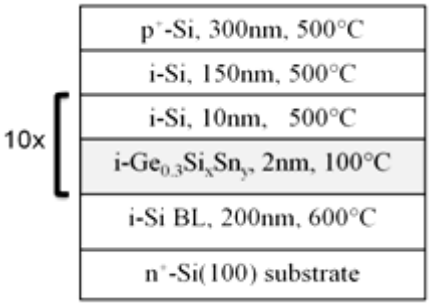


Fig. 5. Scheme of the *p-i-n* structure.

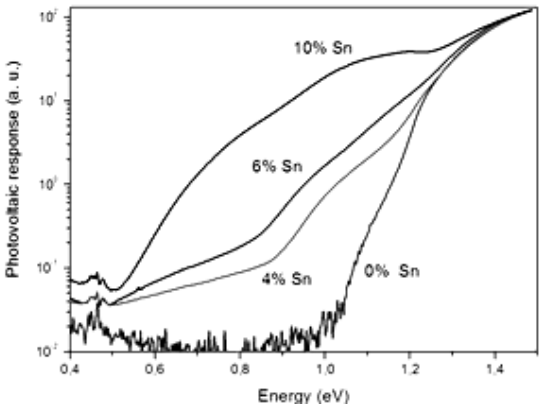


Fig. 6. A series of photoconductivity spectra in the photovoltaic regime at zero bias for the samples with the different Sn content in the *p-i-n* structure.

The photoconductivity spectra were acquired in the photovoltaic regime at zero bias. An increase in photoresponse with is observed as the Sn concentration in the GeSiSn layer increases from 0 to 10%. The maximal photoresponse is at the 10% Sn content and covers the wavelengths from near to mid-IR ranges. The photoconductivity increases by 2–3 orders of magnitude compared to the multilayer structures on GeSi quantum wells.

4. CONCLUSION

Regularities of the formation of multilayer structures with strained pseudomorphous GeSiSn layers without relaxed buffer layers but creating the structures directly on Si were studied for the first time. The obtained TEM and X-ray data proved the crystal perfection of the samples under study. The multilayer periodic GeSiSn/Si heterostructures demonstrated the photoresponse increasing by several orders of magnitude compared to the Sn-free structures at an increase in the Sn content.

Acknowledgments. The work is supported by the Russian Foundations of Basic Research (Projects 16-29-03292, 18-52-41006) and Uzbek-Russian Joint Research (Project MRU-FA-31/2017).

REFERENCES

1. S. Gupta, Y.-Ch. Huang, Y. Kim, E. Sanchez, and K.C. Saraswat, IEEE Electron Device Lett. **34**, 831 (2013).
2. R. Chen, S. Gupta, Y.-Ch. Huang, Y. Huo, C.W. Rudy, E. Sanchez, Y. Kim, T.I. Kamins, K.C. Saraswat, and J.S. Harris, Nano Lett. **14**, 37 (2014).

3. S. Wirths, D. Stange, M.-A. Pampillón, A.T. Tiedemann, G. Mussler, A. Fox, U. Breuer, B. Baert, E. San Andrés, N.D. Nguyen, J.-M. Hartmann, Z. Ikonic, S. Mantl, and D. Buca, ACS Appl. Mater. Interfaces **7**, 62 (2015).
4. S. Wirths, R. Geiger, N. von den Driesch, G. Mussler, T. Stoica, S. Mantl, Z. Ikonic, M. Luysberg, S. Chiussi, J.M. Hartmann, H. Sigg, J. Faist, D. Buca and D. Grützmacher, Nat. Photonics **9**, 88 (2015).
5. J. Kouvetakis, A.V.G. Chizmeshya, J. Mater. Chem. **17**, 1649 (2007).
6. A. Tonkikh, C. Eisenschmidt, V. Talalaev, N. Zakharov, J. Schilling, G. Schmidt, and P. Werner, Applied Physics Letters **103**, 032106 (2013).
7. C. Xu, L. Jiang, J. Kouvetakis, and J. Menéndez, Applied Physics Letters **103**, 072111 (2013).
8. M. Oehme, K. Kostecki, M. Schmid, F. Oliveira, E. Kasper, J. Schulze, Thin Solid Films **557**, 169 (2014).
9. T. Asano, T. Terashima, T. Yamaha, M. Kurosawa, W. Takeuchi, N. Taoka, O. Nakatsuka, and S. Zaima, IEEE **159** (2014) (7th International Silicon-Germanium Technology and Device Meeting (ISTDM)).
10. D. Zhang, L. Jin, J. Li, T. Wen, C. Liu, F. Xu, J. Kolodzey, Y. Liao, Journal of Alloys and Compounds **665**, 131 (2016).
11. S. Gupta, B. Magyari-Köpe, Y. Nishi, K.C. Saraswat, J. Appl. Phys. **113**, 073707 (2013).
12. W. Du, S.A. Ghetmiri, B.R. Conley, A. Mosleh, A. Nazzal, R.A. Soref, G. Sun, J. Tolle, J. Margetis, H.A. Naseem, and S.Q. Yu, Appl. Phys. Lett. **105**, 051104 (2014).
13. C.L. Senaratne, J.D. Gallagher, T. Aoki, J. Kouvetakis, Chem. Mater. **26**, 6033 (2014).
14. S. Wirths, D. Buca, S. Mantl, Progress in Crystal Growth and Characterization of Materials (2015); Advance online publication. doi: 10.1016/j.pcrysgrow.2015.11.001.
15. A.E. Dolbak, B.Z. Olshanetsky, Cent. Europ. Journal of Physics **6**, 634 (2008).
16. A.I. Nikiforov, V.I. Mashanov, V.A. Timofeev, O.P. Pchelyakov, H.-H. Cheng, Thin Solid Films **557**, 188 (2014).
17. A. Harwit, P. Pukite, J. Angilello, and S. Iyer, Thin Solid Films **184**, 395 (1990).
18. J. Tolle, A. Chizmeshya, Y. Fang, J. Kouvetakis, V. D'Costa, C. Hu, J. Menendez, and I. Tsong, Appl. Phys. Lett. **89**, 231924 (2006).
19. R.R. Lieten, J.W. Seo, S. Decoster, A. Vantomme, S. Peters, K.C. Bustillo, E.E. Haller, M. Menghini, J.P. Locquet, Appl. Phys. Lett. **102**, 052106 (2013).
20. J. Xie, J. Tolle, V. D'Costa, A. Chizmeshya, J. Menendez, and J. Kouvetakis, Appl. Phys. Lett. **95**, 181909 (2009).
21. T. Tsukamoto, N. Hirose, A. Kasamatsu, T. Mimura, T. Matsui, and Y. Suda, Applied Physics Letters **106**, 052103 (2015).
22. K. Ueda, K. Kinoshita, M. Mannami, Surface Science **145**, 261 (1984).